Association-Matrix-Based Sample Consensus Approach for Automated Registration of Terrestrial Laser Scans Using Linear Features

Kaleel Al-Durgham and Ayman Habib

Abstract

This paper presents an approach for the automatic registration of terrestrial laser scans using linear features. The main contribution here is introducing a new matching strategy that uses an association matrix to store information about candidate matches of linear features. The motivation for this work is aiding the 3D modeling of industrial sites rich with pole-like features. The proposed matching strategy aims at establishing hypotheses about potential minimal matches of linear features that could be used for the estimation of the transformation parameters relating the scans; then, quantifying the agreement between the scans using the estimated transformation parameters. We combine the association matrix and the well-known RANSAC approach for the derivation of conjugate pairs among the two scans. Rather than randomly selecting the line pairs as in the RANSAC-based registration, the association matrix guides the process of selecting the candidate matches of linear features. Experiments are conducted using laser scanning data of an electrical substation to assess the performance of the proposed association-matrix-based sample consensus approach as it compares to the traditional RANSAC-based procedure. The association-matrix-based approach showed consistent tendency of bringing up the correct matches first before the RANSAC-based registration.

Introduction

The ability of collecting dense 3D spatial data without the need for the direct contact together with the low operational cost with few crew members encouraged institutions and individuals to utilize terrestrial laser scanning systems in wide range of applications such as digital building model generation, industrial site modeling, cultural heritage documentation, and other civilian and military applications. The acquisition of several laser scans with significant overlap is one of the fundamental requirements to guarantee full coverage of the site of interest and to attain more details than what could be achieved from a single scan. The raw outcome of a single terrestrial scan is a cloud of 3D coordinates that are defined with respect to a local coordinate system associated with the scanner's location and orientation. Hence, a registration process has to be performed when dealing with multiple scans in order to align these scans to a common reference frame. A registration process aims at estimating the 3D-Helmert transformation parameters that describe the absolute orientation parameters between the involved scans. The 3D-Helmert transformation parameters include three rotation angles, three translations, and a scale factor. For a well-calibrated laser scanner, the scale factor is considered unity since the laser ranging principle provides the true scale. To date, a vast amount of research work with various methodologies has been conducted on the registration of laser scans (Liang *et al.*, 2014; Theiler and Schindler, 2012; Yao *et al.*, 2010). According to Habib and Al-Ruzouq (2004), a registration process should address four issues: (a) The registration primitives which are the conjugate features within the scans that can be used to solve for the transformation parameters. These primitives could be points, 3D lines, and/or planes; (b) The transformation parameters relating the reference frames of the involved datasets; (c) The similarity measure, which is the mathematical constraint that describes the coincidence of conjugate primitives after the registration process; and (d) The matching strategy, which represents the guiding framework for the automatic registration process. Registration algorithms can be divided into three main categories: (a) point-based algorithms that use points as the registration primitives; (b) feature-based algorithms that use other geometric features as the registration primitives; and (c) direct georeferencing algorithms that incorporate additional sensors such as *GNSS* and *INS* with the laser scanner. The point-based algorithms are usually used to establish the fine alignment between the overlapping scans, while the feature-based and the direct georeferencing registration algorithms target the problem of establishing the coarse alignment between the scans. The well-known Iterative Closest Point (*ICP*) (Besl and McKay, 1992; Chen and Medioni, 1992; Zhang, 1994) is an example of the most commonly used point-based registration algorithm, which minimizes the point-to-point distance in the overlapping area between the different scans. The Iterative Closest Patch (*ICPatch*) (Habib *et al.*, 2010) is a variant of the *ICP* where points in one scan and a triangular irregular network in another scan serve as the registration primitives. The transformation parameters are estimated by minimizing the sum of the squared normal distances between the conjugate point-patch pairs. Another derivative of the *ICP* is the Iterative Closest Projected Point (*ICPP*), which aims at minimizing the distance between a point in one scan and its projection on the plane defined by the closest three points in the other scan (Al-Durgham and Habib, 2013). Point-based registration algorithms were proven to be accurate. However, in order to establish the primitives correspondence (i.e., point to its nearest point in another scan or point to its nearest patch), a coarse alignment of the scans being registered is required. In

Kaleel Al-Durgham is with the Digital Photogrammetry Research Group (DPRG), Department of Geomatics Engineering Schulich School of Engineering, University of Calgary (kmaldurg@ucalgary.ca).

Ayman Habib is with Lyles School of Civil Engineering, Purdue University (ahabib@purdue.edu).

Photogrammetric Engineering & Remote Sensing
Vol. 80, No. 11, November 2014, pp. 1029–1039.
0099-1112/14/8011–1029

doi: 10.14358/PERS.80.11.1029

other words, the point-based registration approaches should start from very good approximations of the transformation parameters (Besl, 1988). Therefore, a wide variety of research efforts have been focusing on automating the initial alignment (i.e., coarse alignment) between the laser scans as a preparatory step to applying the point-based registration algorithms. For instance, shape descriptors such as the 3D Scale Invariant Feature Transforms (SIFT) operators were used to track correspondences between rigid and non-rigid meshes (Zaharescu *et al.*, 2009). Least squares image-matching techniques can be extended to 3D least squares matching for establishing feature-to-feature correspondence between 3D surfaces (Akca, 2010). Other matching techniques involve extracting corresponding primitives from panoramic reflectance images, which are known in literature as Images-Based Registration (*IBR*) (Kang *et al.*, 2009). Matabosch *et al.* (2005) surveyed several techniques such as Spin Images, Point Signature, and the RANdom SAmple Consensus approach (*RANSAC*) for identifying possible congruent points, curves, or surfaces. These techniques are computationally expensive since the feature extraction includes transforming the raw point cloud into another domain (i.e., images or meshes) and then further steps are required to identify matching primitives. Other feature-based registration algorithms utilize geometric primitives such as lines, planes, spheres, and other higher order primitives to establish the initial alignment between the laser scans. These primitives, which can be automatically extracted, provide a strong link between laser scans and have been proven as good registration primitives that are robust to the quality of the initial approximations of the transformation parameters. Rabbani and vanden Heuvel (2005) used planes, cylinders, and spheres as registration primitives. Their methodology of finding possible conjugate features was complemented by geometric constraints. Jaw and Chuang (2008) showed that linear and planar primitives offer reliable accuracy for the registration of neighboring laser scans. Yao *et al.* (2010) proposed a comprehensive work for automating the laser data registration using linear and planar primitives. They developed a *RANSAC*-based algorithm to register laser scans in a pairwise fashion (i.e., two scans are registered at a time). Their algorithm is based on measures that describe the shape and distribution of groups of linear and planar primitives in 3D space. It is reported that this method is sensitive to the presence of repetitive patterns, and the results of outdoor scene registration usually failed. One can argue that linear features are the best choice of geometric primitives for the automatic registration due for the following reasons: (a) they are the most common geometric primitives that would exist in laser data covering urban scenes or industrial sites; (b) they can be represented with few parameters that will help in simplifying the fundamental tasks of aligning the scans in 3D space; and (c) 3D linear primitives provide a strong tie between photogrammetric and laser data, which could be quite useful for subsequent integration activities (i.e., they can be used for further alignment of photogrammetric and laser scanning data) (Canaz, 2012). One should note that the aforementioned reasons are valid for planar and linear features. Nevertheless, given that the laser scanners provide true scale and assuming no systematic errors in the laser data, a minimum of one corresponding pair of non-parallel lines is enough for estimating the six transformation parameters relating two laser scans (i.e., three shifts and three rotation angles) (Renaudin *et al.*, 2011). On the other hand, a minimum of three corresponding pairs of non-parallel planar features are required for the estimation of such parameters (Dold and Brenner, 2006). From a matching strategy point of view, the search for two conjugate linear features in two scans is much easier than searching for three conjugate planar features.

Some of the feature-based registration algorithms utilize artificial features (targets) for the registration of terrestrial laser scans. These features are specially designed to allow for their automatic recognition from the laser scans. A human interaction is required to localize the targets within the scanner field of view, which can be restricted by the field access limitations. In addition, the initial alignment between the involved scans is manually achieved by visualizing the scans using specially-developed software (Liang *et al.*, 2014). In the direct georeferencing registration methods, integrated *GNSS/INS* units are used to derive the absolute position and orientation of the laser scanner relative to the mapping frame and thus establish the coarse alignment among the scans. The direct georeferencing methods are applicable for airborne laser scanners (Habib *et al.*, 2010), mobile terrestrial laser scanners (Wen *et al.*, 2014), and static terrestrial laser scanners (Wilkinson *et al.*, 2010). Due to the fact that the incorporation of direct georeferencing sensors impose additional expenses to the scanning system, the direct georeferencing methods are not preferable for most of static terrestrial laser scanning applications.

This paper introduces a new approach for the automatic registration of terrestrial laser scans using linear features. To address this topic, we started with a brief review of relevant literature. Afterwards, the proposed methodology for using linear features to establish the automatic registration framework is outlined. The proposed methodology is evaluated in the experimental results section, where a comparison between the association-matrix-based sample selection and the *RANSAC*-based approaches is established. Finally, the paper presents some conclusions and recommendations for future work.

Methodology

This section explains the proposed methodology for the automatic registration of overlapping scans using linear features. First, we illustrate the procedure for extracting the linear features from laser scans. The minimum required number of linear features to estimate the transformation parameters between two laser scans and the utilized mathematical model are briefly discussed. Invariant characteristics of a 3D line pair that help in identifying hypothesized matches of linear features between the scans are then introduced. Afterwards, we summarize the *RANSAC*-based procedure that could be used to establish the matching strategy. Finally, the adaptation of the *RANSAC* to the association-matrix-based sample consensus approach is introduced.

Linear Features Extraction

The extraction of linear features from terrestrial laser scans can be achieved indirectly by segmenting the point cloud into planar and non-planar surfaces and thereafter determining virtual/physical linear features through the intersection of neighboring planar surfaces (Lari *et al.*, 2011). In this research, we are dealing with the registration of industrial scenes that contain several pole-like features. Therefore, we utilized a region-growing approach that was developed for the direct extraction of pole-like features from terrestrial laser scans where these features can be fitted as 3D lines or cylinders. The conceptual basis of this approach is the utilization of the minimum parameterization of linear/cylindrical features during the region-growing stage. This parameterization model was introduced by Lari and Habib (2013) to avoid singularities during the fitting process. The approach uses the Principal Component Analysis (*PCA*) to identify potential seed points that belong to pole-like features within the laser scan. First, we estimate the initial parameters representing the linear/cylindrical feature at the vicinity of the seed points. Through the *PCA*, the eigenvector corresponding to the largest eigenvalue provides the approximate direction of the linear/cylindrical feature. The other initial characteristic

attributes describing the feature (i.e., location of a point along the feature and the radius of the cylinder) are then estimated while considering the local point density variation. Second, starting from a single seed point, the neighboring points which belong to the same feature will be sequentially identified by checking point-to-line/point-to-cylinder surface normal distance. The 3D line/cylinder parameters that are associated with a seed point are refined iteratively using a least squares fitting procedure. Afterwards, the points in a single feature are projected onto the line/cylinder axis to determine the extreme points along that feature. Finally, the extreme points are used as descriptors of the linear/cylindrical features within the scan. Henceforth, the linear features and the axes of the cylindrical features are used as the registration primitives.

Linear Features Requirements for the Estimation of Transformation Parameters

A 3D linear feature has four degrees of freedom (Roberts, 1988). Therefore, a single straight line that could be identified in two terrestrial laser scans enables the estimation of four transformation parameters relating these scans (i.e., two shifts across the line direction and two rotation angles defined by the line direction). Another parallel line would allow for the estimation of the relative scale between the two scans as well as the rotation across the lines (i.e., the seven transformation parameters with the exception of the shift along the lines' direction can be estimated using two parallel lines). Two coplanar and non-parallel lines would allow for the estimation of the three shifts and three rotation angles between the two scans (i.e., only the scale parameter cannot be estimated using such lines). Therefore, two non-coplanar lines which can be identified in both scans will allow for the estimation of the relative scale, three shifts, and three rotation angles between the two scans. Thus, in the absence of systematic errors and knowing that laser ranges define the true scale, the minimum number of linear features for the estimation of the three rotation angles and the three translations are two non-parallel lines. Figure 1 shows the defined shifts and rotations using two non-parallel lines (e.g., the lines $\vec{a}$ and $\vec{b}$).

Due to the nature of the linear feature extraction procedure, the definition of the line end-points is quite arbitrary (i.e., conjugate linear features will not have conjugate ending points). As for the incorporation of linear features for the estimation of transformation parameters, one could implement one of the following procedures: line-based approach (Habib *et al.*, 2005) or point-based approach through a weight-modification process (Renaudin *et al.*, 2011). In this work, we used the weight modification process proposed by Renaudin *et al.* (2011) since it is much easier in terms of implementation. Please refer to Renaudin *et al.* (2011) for more detailed information about how the modified weight can be used to deal with non-conjugate points along corresponding lines for the estimation of the unknown transformation parameters.

Invariant Characteristics of a 3D Line Pair

The conceptual basis for the identification of conjugate linear features in two neighboring scans is utilizing invariant characteristics among conjugate linear features. First, the angular deviation between two lines is invariant to shift, rotation, and scale differences between two neighboring scans. Figure 2a shows the angular deviation (θ) between two 3D lines (e.g., $\vec{a}$ and $\vec{b}$). Second, in the absence of scale difference between two neighboring scans, the spatial separation (Figure 2b) between lines $\vec{c}$ and $\vec{d}$ is invariant to shift and rotation differences. The spatial separation (S) represents the length of the common perpendicular line between two lines in 3D. The algebraic equations for deriving the angular deviation and spatial separation between two 3D lines can be found in Al-Durgham *et al.* (2013).

The angular deviation and spatial separation values between the constituents of a line pair in one scan are used to identify its hypothesized conjugate pair in another scan

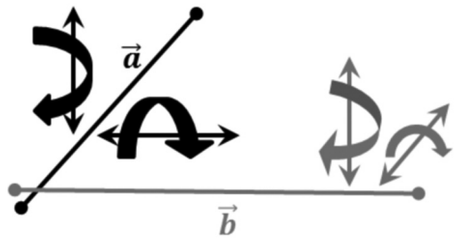

Figure 1. Established shifts (double-sided straight arrows) and rotations (curved arrows) by two non-parallel linear features ($\vec{a}$ and $\vec{b}$).

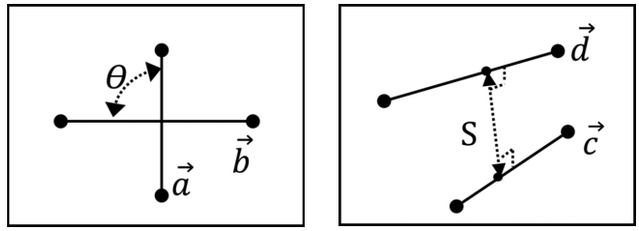

Figure 2. (a) Angular deviation between the lines ($\vec{a}$ and $\vec{b}$), and (b) spatial separation between two lines ($\vec{c}$ and $\vec{d}$) in 3D.

(candidate match). For example, if the angular deviation and spatial separation between lines $\vec{a}$ and $\vec{b}$ in the first scan are similar to those between lines $\vec{c}$ and $\vec{d}$ in the second scan, then one can assume that these line pairs are conjugate to each other. In this case, "similar" means that they have close values within predefined thresholds, which depend on the noise level in the data as well as the accuracy of the feature extraction procedure. Since this approach is aiming at the coarse alignment of two scans, the outcome of the registration process would not be too sensitive to the utilized values of these thresholds. In this work, the thresholds are selected as 5° for the angular deviation and 0.1 m for the spatial separation.

One should note that there will be two ambiguous matches in this case (i.e., line $\vec{a}$ in the first scan could be conjugate to either line $\vec{c}$ or line $\vec{d}$ in the second scan, while line $\vec{b}$ in the first scan would correspond to either line $\vec{d}$ or line $\vec{c}$ in the second scan). One should also note that the radii of the cylindrical features could be used for the identification of possible correspondences between the scans. However, the accuracy of the estimated radii is not high enough for this purpose, since the laser scan from a given vantage point would not be able to provide a complete coverage of the cylinder surface.

If we have n linear features in the first scan and m linear features in the second scan, we will have $n\times(n-1)/2$ and $m\times(m-1)/2$ line pair combinations in each scan, respectively. Due to the fact that a hypothesized match between two pairs in the two scans is equivalent to two possible matches between the individual linear features, the total number of possible pair combinations will be equal to the number of line combinations in the first scan multiplied by twice the number of combinations in the second scan according to Equation 1.

$$N_p = n(n-1)/2 \times m(m-1) \quad (1)$$

where, N_p is the total number of possible pair combinations.

By comparing the angular deviation and spatial separation values, we can determine the total number of combinations that represent candidate matches and thus filter-out incompatible pairs from the possible pair combinations. In this

case, the total number of candidate matches - which will be denoted as N_c in this paper will be less than the total number of possible pair combinations (N_p).

RANSAC Approach

In our previous work (Al-Durgham *et al.*, 2013), we introduced a *RANSAC*-based approach to establish the correspondence between the linear features in overlapping scans. In the *RANSAC*-based approach, a randomly selected pair from the first scan is considered as a candidate match to a randomly selected pair in the second scan if they have similar angular deviation and spatial separation values. Then, the hypothesized pairs are used to estimate the transformation parameters relating the two scans provided that the linear features in either of these pairs are not parallel to each other. Following the estimation of the transformation parameters from a given pair, we check the compatibility among the remaining linear features (i.e., identify which linear features in the two scans would become collinear following the application of the estimated transformation parameters) as well as the number of matched points between the scans through the *ICPP* registration procedure (Al-Durgham and Habib, 2013). The process of random selection of pairs of linear features from both scans, estimation of the transformation parameters, and identification of compatible matches of linear features and points between the scans following the registration are repeated until a sufficient number of hypothesized pairs (i.e., trials) is investigated. The matching pair that results in the largest number of compatible points between the scans following the registration would be considered as a true match and the transformation parameters can be finally estimated using the compatible linear features and then refined through the *ICPP*.

As was mentioned in the previous paragraph, the *RANSAC*-based approach does not perform exhaustive investigation of all candidate matching pairs in the two scans. Rather, it only investigates a predetermined number of candidate matching hypotheses (trials). We adapted the formula that was provided by Derpanis (2010) for the derivation of the minimum number of required *RANSAC* trials. Such formula derives the number of required *RANSAC* trials based on a probabilistic estimation to guarantee that at least one correct draw of a true matching pair (inlier pair) has been selected from the candidate matching pairs (N_c). For further explanation, first we start by establishing the probability value (P_T) of having one correct draw of a true matching pair from the candidate matches according to Equation 2. An important note is that if there are (x) conjugate lines (inlier features) within the overlapping scans, the number of inlier pairs (N_i) can be determined as in Equation 3.

$$P_T = N_i \,/\, N_c \tag{2}$$

$$N_i = x(x-1)/2 \tag{3}$$

Assuming that (P_i) is the probability of having at least one correct draw after (N) trials, one can derive the expression in Equation 4, which represents the probability of not having any correct draws after (N) trials. Based on Equation 4, the number of required trials (N) can be determined as in Equation 5 provided that the probability (P_i) is usually set to a high value (e.g., 0.99).

$$1 - P_i = (1 - P_T)^N \tag{4}$$

$$N = \frac{\log(1-P_i)}{\log(1-P_T)} = \log(1-P_i) \,/\, \log\left(1-\frac{N_i}{N_c}\right) \tag{5}$$

One should note that the number of inlier pairs (N_i) is not known *a priori* since we do not know the number of conjugate linear features in the two scans. Therefore, following the estimation of the transformation parameters using a matching pair, we use the transformation parameters to transform the linear features in one scan to the reference frame of the other scan. And then, we identify which linear features from the different scans will become collinear. In particular, the number of linear features that will become collinear is used as an indication for the number of conjugate features within the scans. The number of compatible features will be then used to determine the number of inlier pairs. In other words, the number of required trials will be estimated after each matching-pair draw by updating the number of inlier pairs. The estimated value for the necessary trials from a previous draw will be updated if and only if larger number of inlier features has been established, since a larger number of inlier features would lead to fewer numbers of trials. In this regard, one should note that having fewer number of inlier features in the earlier draws of the sample selection process would lead to having higher number of trials to achieve the desired probability of having at least one correct draw of a true matching pair from the available candidate matches.

Association-Matrix-Based Sample Consensus Approach

In this work, we will combine what will be denoted as "association matrix" and *RANSAC* for the derivation of conjugate pairs among the two scans and estimation of the transformation parameters relating them. However, rather than randomly selecting the line pairs as in the *RANSAC*-based procedure, we restrict the sample draws by utilizing the association matrix that will guide the process of selecting candidate matches of linear features. This approach is denoted as the "association-matrix-based sample consensus."

Building the Association Matrix

The association matrix in this context is a mean to store information about probable matches of linear features. A voting scheme is followed to build the matrix based on the angular deviation and spatial separation values between linear features. The association matrix is an $n \times m$ matrix where n is the number of the linear features in the first scan, and m is the number of linear features in the second scan. A non-zero element in the i^{th} row and j^{th} column of the association matrix indicates that a hypothesized match can be made between the i^{th} line in the first scan and the j^{th} line in the second scan. To establish the correspondences between the linear features in the overlapping scans, we start by constructing an association matrix, whose elements are initialized to zero. Then, we identify the pairs that have similar angular deviation and spatial separation values in both scans. For each of these pairs, two ambiguous matches (as previously explained) will exist. Therefore, we increment the corresponding elements in the association matrix for all the possible matching options for that matched pair. This process is repeated until all the pairs with similar angular deviation and spatial separation in both scans are considered. Since conjugate linear features in two scans are expected to appear several times among pairs of lines with equivalent angular deviation and spatial separation, these lines would end up with higher votes in the data association matrix. The best case scenario would lead to an association matrix that could be used for unique identification of corresponding features in overlapping scans. Starting from the match with the highest vote and proceeding in a descending order while avoiding one-to-many matches (i.e., we cannot consider two matches in the same row or column), we can identify the correspondences between the linear features in the two scans. Therefore, such a characteristic would allow us to identify conjugate linear features in the two scans.

Table 1. Spatial Separation "S" and Angular Deviation "Θ" Values Between All Possible Pairs Of Linear Features In Scan 1

Line ID	a1	a2	a3	a4
a1	-	S = 0 m	S= 0 m	S= 0 m
a2	Θ = 90°	-	S= 0 m	S= 0 m
a3	Θ = 60°	Θ = 45°	-	S= 0 m
a4	Θ =90°	Θ = 90°	Θ = 35°	-

Table 2. Association Matrix Initialization

Line ID	b1	b2	b3	b4
a1	0	0	0	0
a2	0	0	0	0
a3	0	0	0	0
a4	0	0	0	0

Table 3. Adding A Single Vote in the Corresponding Matching Positions of Line Pairs (a1, a2) and (b1, b2)

Line ID	b1	b2	b3	b4
a1	1	1	0	0
a2	1	1	0	0
a3	0	0	0	0
a4	0	0	0	0

Table 4. Candidate Matches of Linear Features

Pairs	b1-b2	b1-b3	b1-b4	b2-b3	b2-b4	b3-b4
a1-a2	✓		✓		✓	
a1-a3		✓				
a1-a4	✓		✓		✓	
a2-a3				✓		
a2-a4	✓		✓		✓	
a3-a4						✓

Table 5. Final Association Matrix

Line ID	b1	b2	b3	b4
a1	5	4	1	4
a2	4	5	1	4
a3	1	1	3	1
a4	4	4	1	5

In order to provide an example for the application of the sequential procedure for building the association matrix and identification of conjugate features, we will introduce a simulated scenario of extracted linear features in two scans. Figure 3 shows two simulated laser scans over a building model and the extracted linear features, where the lines (a1, a2, a3, and a4) are conjugates to lines (b1, b2, b3, and b4), respectively.

The angular deviation and spatial separation values between all possible pairs of linear features in Scan 1 are illustrated in Table 1. The upper triangle of the table contains the spatial separation values between the line pairs, and the lower triangle contains the angular deviation values. All the possible pairs of linear features in Scan 2 will have similar angular deviation and spatial separation values to those in Table 1 since the lines in both scans follow the same pattern.

The procedure for building the association matrix for the provided scenario in Figure 3 can be summarized in the following steps:

1. Construct a 2D matrix with number of rows equal to the number of linear features in the first scan, and number of columns equal to the number of linear features in the second scan. All the elements of the association matrix are set to zero as shown in Table 2. Starting from the first candidate match of line pairs, we add a single vote for corresponding elements in the association matrix. For example, the lines pair (a1, a2) is a candidate match to the lines pair (b1, b2) since they have similar angular deviation and spatial separation values. Considering that line a1 in the first scan could be conjugate to either line b1 or line b2 in the second scan while line a2 in the first scan could correspond to either line b2 or line b1 in the second scan, we add a single vote for the elements corresponding to the following matches: (a1, b1), (a1, b2), (a2, b1), and (a2, b2) in the association matrix as shown in Table 3.
2. Considering all candidate matches for the line pairs that are summarized in Table 4, we increment the votes for the four elements corresponding to the constituents of a given candidate match (i.e., the line pairs that exhibit similar angular deviation and spatial separation). The resulting association matrix for the provided example after considering all the candidate matches in Table 4 is shown in Table 5.

Based on Figure 3, we can visually identify that line a1 is conjugate to line b1, line a2 is conjugate to line b2, and so on for lines (a3, b3) and (a4, b4). The association matrix in Table 5 can be used to derive the correct conjugates of linear features by checking the final votes in the association matrix. One can note that the number of votes for the matching pair (a1, b1) is the highest-unique number of votes within the row

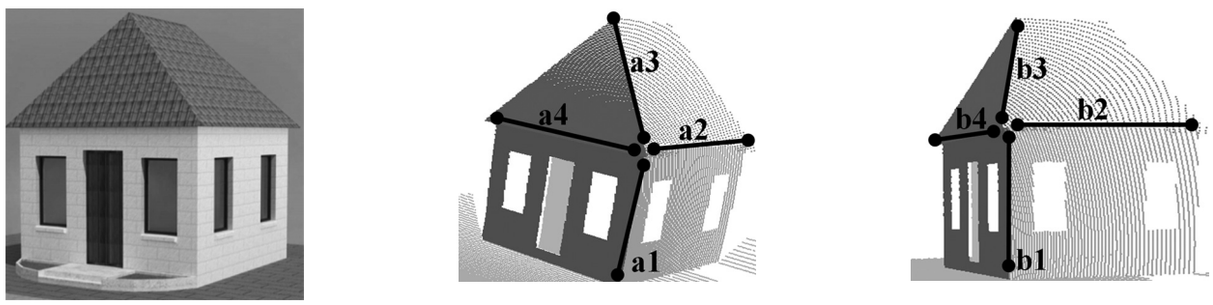

Figure 3. Extracted linear features from two laser scans taken over a building: (a) Building under consideration, (b) Scan 1 and the extracted linear features (a1, a2, a3, and a4), and (c) Scan 2 and the extracted linear features (b1, b2, b3, and b4).

a1 and the column b1. Similarly, the same observation is valid for the matching pairs (a2, b2), (a3, b3) and (a4, b4). At this stage, we can define the correct correspondence among the linear features as the elements in the association matrix that have the highest-unique number of votes within the column and row where these elements reside. From an implementation point of view, we can start with the hypothesized match that has the highest vote in the association matrix as the first established match. Since in this approach we will not allow one-to-many matches, the remaining elements in the respective row and column of that match are set to zero (i.e., we will not allow a linear feature in the first scan to correspond to more than a single line in the second scan). The same process would proceed by considering the subsequent highest votes in a descending order within the association matrix.

In some situations, a laser scan might contain a pattern of linear features that is similar to a non-conjugate pattern of linear features in another scan. This situation will lead to a matching ambiguity in the association matrix. Figure 4 shows an example of such scenario that occurs in a real dataset collected in an electrical substation. As can be seen in this figure, the lines (a1, a2, a3, and a4) form a pattern similar to the lines (b1, b2, b3 and b4), and they are conjugate. Also, the lines (a1, a2, a3, and a4) form a pattern similar to the lines (b5, b6, b7, and b8) but they are non-conjugate.

After following the proposed procedure of building the association matrix for the scenario in Figure 4, one would obtain the association matrix in Table 6.

Due to the similar angular deviation and spatial separation values between conjugate and non-conjugate line pairs within these patterns, using the association matrix in Table 6 to establish the correspondence will face an ambiguity. In this case, there is no element in this matrix that satisfies the condition of having the highest-unique number of votes within the corresponding row and column of that element. For example, the highest number of votes (which is 9) is repeated in two elements (i.e., a1, b1 and a1, b5). In this case, two ambiguous matches exist and we cannot determine if line a1 is conjugate to b1 or to b5. In a similar manner, there are ambiguous matching options for all the other lines. Therefore, in the next subsection, we will introduce a general methodology to identify candidate linear feature matches based on the vote information within the association matrix.

Table 6. Association Matrix for the Linear Features in Figure 4 Exhibiting Matching Ambiguity

Line ID	b1	b2	b3	b4	b5	b6	b7	b8
a1	9	3	3	3	9	3	3	3
a2	3	4	3	3	3	4	3	3
a3	3	2	3	2	3	2	3	2
a4	3	3	3	4	3	3	3	4

Identifying Potential Linear Feature Matches through the Association Matrix: To deal with ambiguous matching scenarios that might happen within the association matrix, we designed a general methodology to identify probable candidate matches of linear feature through the association matrix. For this purpose, we would follow a strategy that bears some similarity to the *RANSAC* procedure. However, rather than randomly selecting some pairs from possible matching pairs, we will use the data association matrix to select the potential matching pairs for identifying the inliers consensus. The impact of using the association matrix is reducing the number of trials to achieve the solution with the highest number of inlier features/pairs. The association-matrix-based sample selection methodology can be summarized as follows:

1. Identify the highest vote in the association matrix. If the highest vote appears more than once in the association matrix, one can randomly pick any of these matching hypotheses corresponding to that vote.
2. To complete the pair of needed lines for the estimation of the transformation parameters, we pick the matching element corresponding to the second highest vote. The selected pairs by the highest and second highest votes should satisfy three conditions. First, since we do not allow one-to-many matches, the second highest vote should not be located along the same row or column of the matching hypothesis corresponding to the highest vote. Second, the established matches by the highest and second highest votes should be only considered when the angular deviation and spatial separation between the two linear features in the first scan are similar to those associated with the hypothesized matches in the second scan. Third, the defined pairs by the highest and second highest votes should not be parallel to each other to allow for reliable estimation of the six transformation parameters relating the two scans.
3. Use the established matches in steps 1 and 2 to determine the transformation parameters as well as the number of inlier features (i.e., compatible linear features according to the estimated transformation parameters). Use the estimated inlier pairs to update the number of trials to achieve the required probability of having at least one correct draw of conjugate features from the available linear features in the two scans as per Equation 5.
4. If a certain number of compatible matches of linear features are identified, all the compatible matches are used to estimate a new set of transformation parameters, which are finally refined through an *ICPP* procedure.

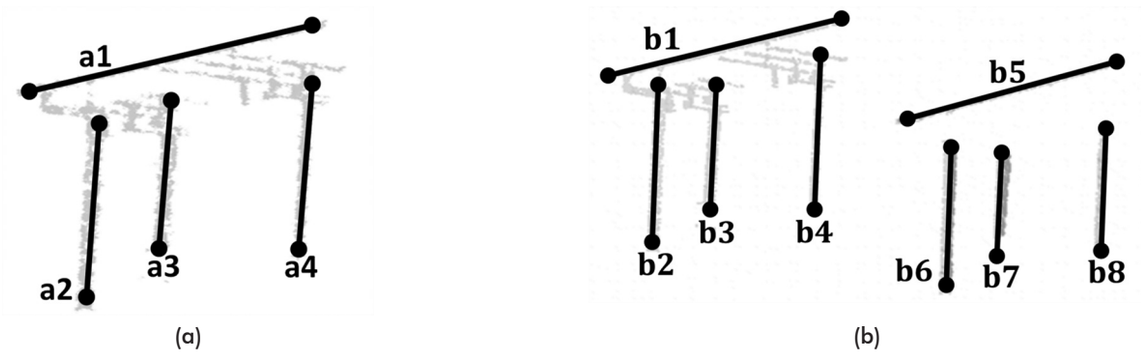

Figure 4. Extracted linear features from two laser scans collected in an electrical substation: (a) Scan 1 and the extracted linear features (a1, a2, a3, and a4), and (b) Scan 2 and the extracted linear features (b1, b2, b3, b4, b5, b6, b7, and b8).

5. After considering the hypothesized matches by the highest and second highest votes, one would proceed with another matching hypothesis that is formed by the highest and third highest votes while considering the three conditions in step 2. These pairs are used to estimate the transformation parameters, determine the number of inlier linear features, determine the number of inlier pairs, and update the number of trials needed to achieve the set probability of having at least one correct draw which can be set to 0.99.
6. Step 5 is repeated while considering the highest vote together with the remaining highest votes in a descending order.
7. After considering all the possible matches involving the highest vote in the association matrix, the vote at this location is set to zero (i.e., this potential match will not be considered any further). Then, steps 1 to 6 are repeated while considering the new highest vote in the updated association matrix (i.e., after setting the original highest vote to zero).
8. Steps 1 to 7 are repeated to consider all possible matching pairs in the association matrix until the number of required trials is achieved.
9. Finally, the right set of transformation parameters is selected as the one that provides the largest number of matched points between the scans.

In general, if we consider that we will exhaust all the possible options in the association matrix, the association-based sample consensus approach would not be significantly different from the *RANSAC*-based approach. However, one could argue that the association-based approach would have a higher probability of bringing up a correct match first before the *RANSAC*-based approach. Having a correct match first would lead to a higher number of inlier features/pairs very early in the conducted trials as well as reducing the required number of trials to stop the sample selection process. Moreover, rather than conducting the necessary trials set by Equation 5, we can only conduct a subset of those trials since Equation 5 is based on a random selection of the pairs from the two datasets, which is not the case here.

Experimental Results and Discussion

Dataset Description

Experiments were conducted using a set of seven terrestrial laser scans. The scans are acquired over an electrical substation using the FARO Focus3D S scanner. As shown in Figure 5, the scanning mission is designed to have two central scans (i.e., scans 6 and 7) with significant overlap in between them (roughly 90 percent). The remaining five scans (i.e., scans 1, 2, 3, 4, and 5) are collected at the outer bounds of the field to fully cover the entire site. The outer scans have roughly 50 percent of overlap with the central scans.

The electrical substation contains several pole-like features, which were extracted through the region-growing segmentation procedure to provide the experiment with the required linear features. Plate 1a shows an example of the segmented pole-like features through the region-growing process for a part of the electrical substation. The points of each individual feature are projected onto the feature axis to define the lines (Plate 1b).

We only selected long and precise pole-like features (e.g., linear features more than 1.0 m long with .05 m fitting precision) since those lines will have accurate attributes. Table 7 summarizes the number of selected linear features from each scan that will be used later for the automated registration procedure.

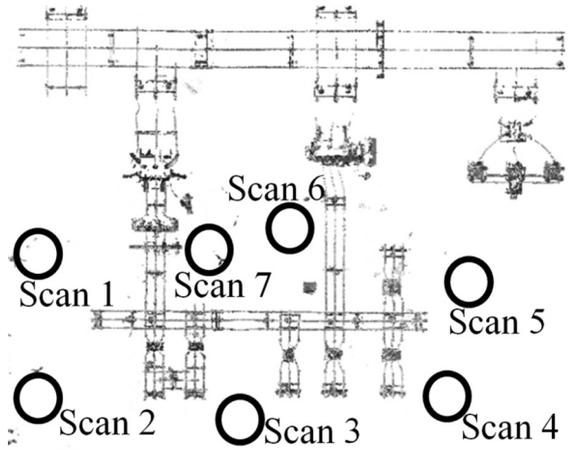

Figure 5. The distribution of the scanner locations within the substation.

Table 7. The number of extracted lines from the different scans

Scan ID	Number of lines
1	33
2	43
3	46
4	33
5	68
6	93
7	85

Results and Discussion

Our objective is to evaluate the performance of the association-matrix-based approach compared to the *RANSAC*-based approach. Therefore, we established two experiments that represent the different approaches to perform the automatic registration for six scan pairs. In the two experiments, the laser scans were selected two at a time where scan 6 was always chosen as the reference scan. For a selected pair of scans, all the possible combinations of linear features (N_p) are established. Then, the candidate matches of line pairs (N_c) between the scans are identified as the ones which share similar angular deviation and spatial separation values. The estimation of the transformation parameters between the scan pairs using linear features requires initial approximations since we are dealing with non-linear model. These approximations are derived by roughly evaluating the position and orientation of the scans with respect to each other. In the first experiment, we used the association-matrix-based approach to guide the process of selecting the candidate matches. All the candidate matches of linear features are used to build the association matrix of the scans being registered. Thereafter, the criteria of selecting candidate matches based on the association vote information is followed. In the second experiment, we applied the *RANSAC*-based procedure to randomly select samples from the candidate matches of linear features. In both experiments, the sample selection process is set to consider all candidate matches of linear features (i.e., draw all candidate matches without applying Equation 5 that should be used to determine the number of sample draws). In order to guarantee a fair comparison between the two approaches, we did not allow the selection of the same sample more than one time for the *RANSAC*-based approach. Since we know the right set of transformation

Table 8. Automatic Registration Outcome for the Ransac and the Association Experiments

Scans ID	Combinations N_p	Candidate matches N_c	Total number of possible trials	Number of solutions	(Association) Number of trials to bring the first correct solution	(RANSAC) Number of trials to bring the first correct solution
6-1	4,517,568	14,828	14,828	31	16	2,394
6-2	7,726,068	26,944	26,944	29	403	665
6-3	8,855,460	60,446	60,446	69	682	294
6-4	4,517,568	13,708	13,708	8	51	364
6-5	19,490,568	86,824	86,824	85	3	12,321
6-7	30,544,920	175,004	175,004	476	1	4,399

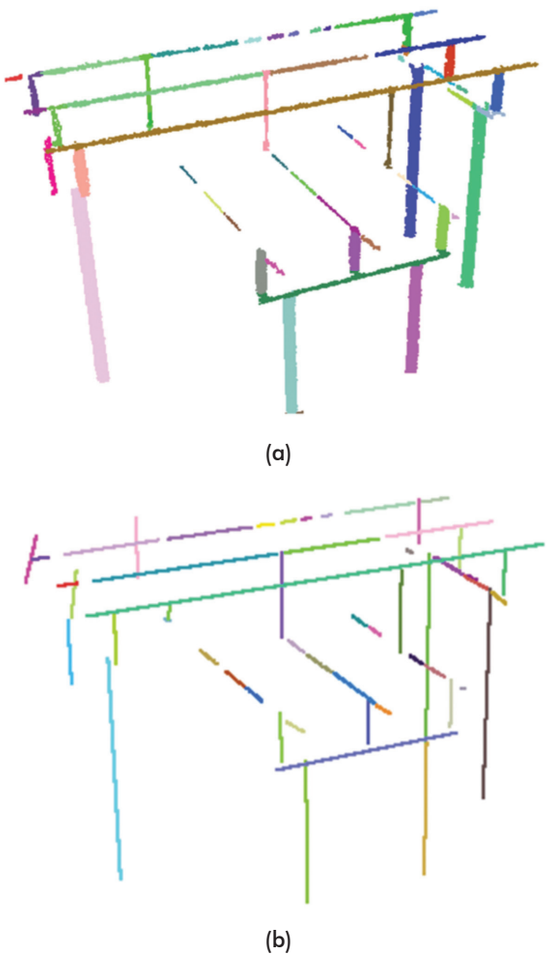

Plate 1. The region-growing segmentation results for a part of the electrical substation: (a) segmented pole-like features, and (b) derived line segments.

parameters relating the scans through a previously established target-based registration process, we identified the right solutions as the ones that fall within a certain buffer from the right set of transformation parameters (e.g., within 0.5 m for the translations and within 0.5° for the rotation angles). Table 8 illustrates the outcome for the two experiments.

A significant variation between the number of solutions and the number of candidate matches is noticeable due to the repetitive patterns of linear features within the electrical substation. In this case, most of the candidate matches will belong to non-conjugate line pairs. By comparing the number of conducted trials to achieve the first correct solution in both experiments (as shown in Table 8), one can note that the association-matrix-based approach will bring the first correct solution earlier than the *RANSAC*-based one in five out of six examined scan pairs; where, the first correct solution was determined earlier in the *RANSAC* procedure for scans 6 and 3, which might occur by chance since the *RANSAC*-based approach is totally random. For further investigation, we kept track the correct solutions occurrence (i.e., solutions that fall within the preset threshold away from the correct solution as determined by the target-based registration) with respect to the conducted trials for all the examined scan pairs. For each of the examined scan pairs, a plot for the conducted trials as a function of the correct solution occurrence is shown in Figure 6. The horizontal axes represent the number of the correct solutions and the vertical axes represent number of conducted trials.

Table 9. Association-Matrix-Based Versus Ransac-Based After Applying the Probability Function

Scans ID	RANSAC total number of conducted trials	Association total number of conducted trials	RANSAC total number of found solutions	Association total number of found solutions
6-1	2,594	1,002	7	21
6-2	2,725	2,725	4	21
6-3	2,928	2,928	10	48
6-4	6,010	6,010	4	8
6-5	12,985	3,460	1	67
6-7	4,399	1,964	2	83

According to Figure 6, the association-matrix-based approach succeeds to bring the solutions with less number of trials when compared to the *RANSAC*-based in the six experiments. In general, a larger number of inlier features will lead to larger number of inlier pairs and hence larger number of votes in the association matrix for the respective element. Based on that, the sample selection through the association-matrix-based approach will have better performance and higher probability for identifying potential matches of linear features. However, random chance might play a role in finding correct solutions first through the *RANSAC*-based approach as in the scan pair 6 and 3 (Figure 6c).The two experiments for evaluating the association-matrix-based against the *RANSAC*-based approach are repeated while applying the probability estimate in Equation 5 to determine the required trials (i.e., not considering the entire candidate matches, which is the default scenario for a *RANSAC* procedure). Here again we did not allow the selection of the same sample more than one time for the *RANSAC* experiment. And in the association experiment, all the candidate matches are used to build the association matrix, and the number of conducted trials is determined by applying the probability function in Equation 5. Table 9 summarizes some of the experiments outcome after applying the probability estimate. By examining Table 9, one can note that the association-matrix-based approach will find more

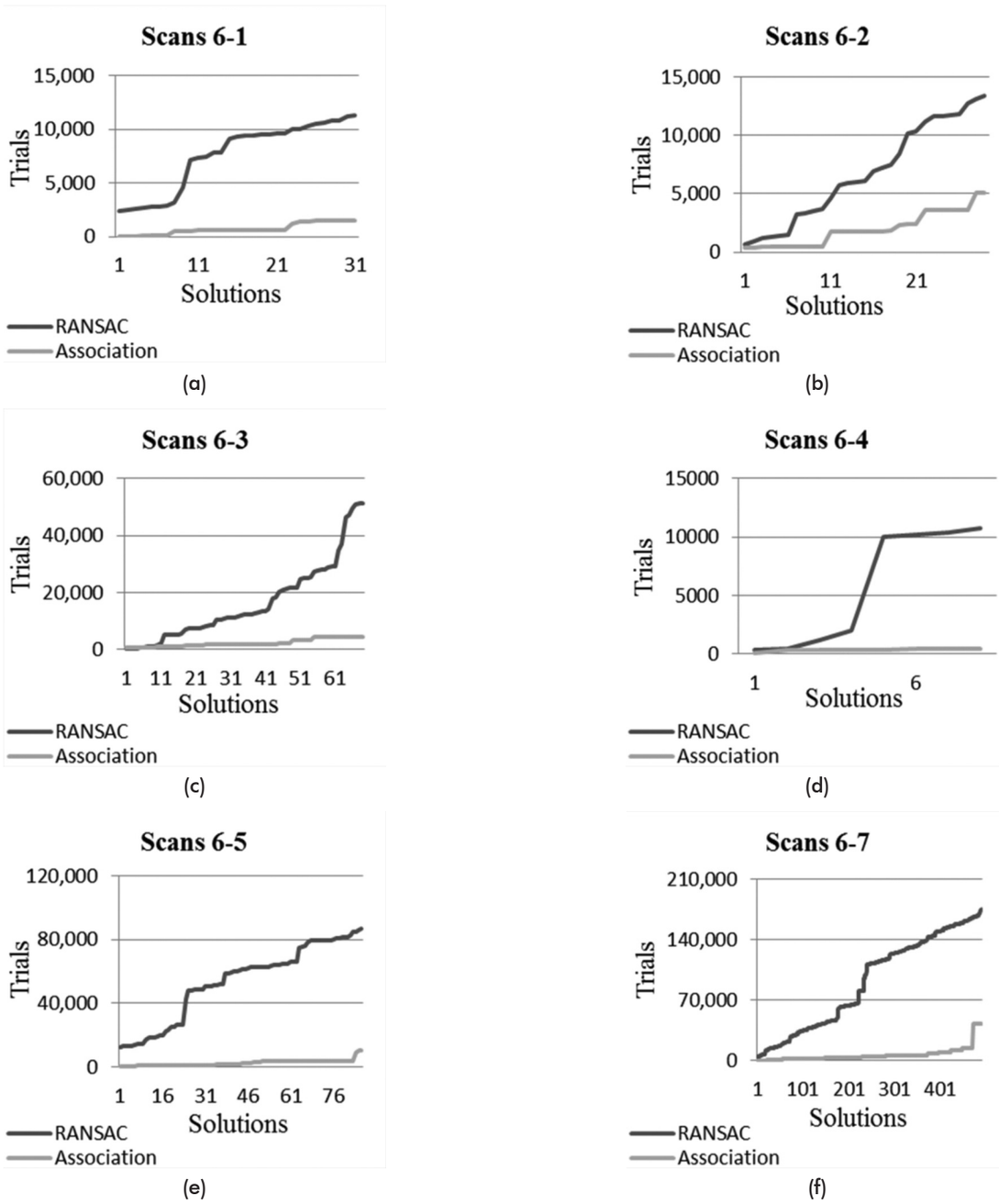

Figure 6. Solutions to conducted trials comparison between the association-matrix-based and RANSAC-based approaches for the selected scan pairs.

solutions with less or equal number of trials when compared to the *RANSAC*-based approach. And hence, rather than conducting the necessary trials set by Equation 5, we can only conduct a subset of those trials since Equation 5 is based on a random selection of the pairs from the two datasets, which is not the case for the association-based-matrix approach. With fewer trials, the association-matrix-based is capable of producing more correct results.

So far, we discussed the advantage of utilizing the association matrix to guide the sample selection process. Regarding the estimated parameters, Table 10 lists the estimated transformation parameters using the identified matches of linear features through the association-matrix-based approach. The refined transformation parameters by the *ICPP* are displayed as well. The estimated transformation parameters from linear features provide a very good initial alignment between the scans, and thereafter the *ICPP* registration starting from these parameters guarantee accurate alignment between the involved scans. Figures 7b and 7c display the registration result for a selected single feature using the line-based transformation parameters and using the *ICPP*-based transformation parameters, respectively. In both figures, different shades of gray indicate different scans. A cross-sectional view is shown in the Figures 8a and 8b for better visualization of the registration results for this feature. As can be seen in Figure 8a, the two parts of the displayed feature that are coming from

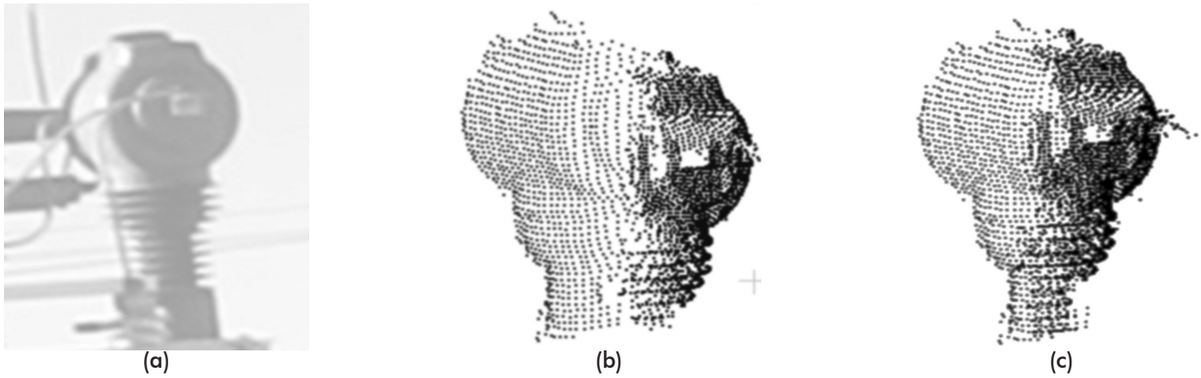

Figure 7. Registration results for a single feature: (a) The feature image, (b) Registration using the estimated transformation parameters through linear features, and (c) Registration using the estimated transformation parameters through the ICPP.

different scans are roughly aligned (coarse registration) using the linear-feature-based approach. Such a result is expected as the derived transformation parameters are impacted by the precision of the linear feature extraction procedure as well as the distribution of the utilized linear features within the overlap area between the scans. In contrast, Figure 8b shows that the *ICPP* has been more successful in establishing more precise alignment of the two scans. This ability is attributed to the fact that all the points in the overlap area between the scans are involved in the derivation of the transformation parameters (i.e., more observations are used for the derivation of the transformation parameters) unlike the case of only using the matched linear features.

Figure 8. Cross-section over the displayed feature in Figure 7: (a) Coarse registration using the estimated transformation parameters through linear features, (b) Fine registration using the estimated transformation parameters through the ICPP.

Table 10. Estimated Transformation Parameters Between the Scan Pairs

Scans ID	Parameters source	$T_x(m)$	$T_y(m)$	$T_z(m)$	$\omega°$	$\varphi°$	$\kappa°$
6-1	Linear features	6.308	-31.352	-0.136	0.034	-0.077	0.284
	ICPP	6.311	-31.361	-0.146	0.045	-0.084	0.268
6-2	Linear features	28.380	-19.889	0.007	0.224	0.218	1.35
	ICPP	28.407	-19.882	0.027	0.201	0.210	1.394
6-3	Linear features	23.100	1.720	0.148	0.173	0.0143	3.561
	ICPP	23.108	1.716	0.147	0.191	0.011	3.549
6-4	Linear features	16.086	24.607	-0.014	-0.41	0.530	2.951
	ICPP	16.117	24.569	-0.027	-0.376	0.561	2.870
6-5	Linear features	-4.274	24.092	0.024	0.223	0.202	-4.652
	ICPP	-4.275	24.089	0.020	0.215	0.196	-4.644
6-7	Linear features	1.926	-9.034	-0.010	0.224	-0.139	2.426
	ICPP	1.930	-9.005	-0.034	0.446	-0.219	2.510

Conclusions and Future Work

The paper outlined a new methodology for the automatic registration of overlapping terrestrial laser scans using linear features. We introduced a new matching strategy by utilizing an association matrix as the means to store potential matches of linear features. The vote information within the association matrix provided a reliable guide for the sample-consensus during the automatic registration process. The advantage of the proposed association-matrix-based sample consensus approach is to avoid selecting random samples as in the *RANSAC*-based and hence accelerate the registration process. Linear features were extracted through a region-growing segmentation procedure. The angular deviation and spatial separation values between the constituents of a line pair helped in identifying candidate matches since these values are invariant with respect to rotation and translation differences between overlapping scans. To achieve the fine alignment between the overlapping scans through the *ICPP*, linear features provided the required quality of approximations for the transformation parameters.

As a future work, the proposed approach will be utilized for the registration of photogrammetric-based point cloud and laser scanning data. We will also investigate the possibility of utilizing a multi-dimensional association matrix to identify compatible matches of linear feature within several laser scans. In addition, we will look into the utilization of the intensity data as an additional attribute for identifying the potential number of hypothesized candidate matches of linear features among the scans.

Acknowledgments

This work is financially supported by the Natural Science and Engineering Council of Canada (*NSERC*-Discovery Grant) as well as a Tecterra Grant (*www.tecterra.com*). The authors are indebted to CANTEGA Technologies (*www.cantega.com*) for supporting the data collection campaign.

References

Akca, D., 2010. Co-registration of surfaces by 3D least squares matching, Photogrammetric Engineering & Remote Sensing, 76 (3):307–318.

Al-Durgham, K., A. Habib, and E. Kwak, 2013. RANSAC approach for automated registration of terrestrial laser scans using linear features, *ISPRS Annals of Photogrammetry, Remote Sensing and Spatial Information Sciences: ISPRS Workshop Laser Scanning 2013*, 11-13 November, Antalya, Turkey, Volume II-5/W2, pp.13–18.

Al-Durgham, M., and A. Habib, 2013. A framework for the registration and segmentation of heterogeneous lidar data, Photogrammetric Engineering & Remote Sensing, 79(2):135–145.

Besl, P., and N. McKay, 1992. A method for registration of 3-D shapes, *IEEE Transactions on Pattern Analysis and Machine Intelligence on Interpretation of 3-D Scenes*, 14(2):239–256.

Besl, P.J., 1988. Geometric modeling and computer vision, Proceedings of the IEEE, 76(8):936–958.

Canaz, S., 2012. *Planar and Linear Feature-Based Registration of Terrestrial Laser Scans with Minimum Overlap Using Photogrammetric Data*, M.Sc. thesis, No. UCGE 20364, University of Calgary, Calgary, AB, Canada, 142 p.

Chen, Y., and G. Medioni, 1992. Object modelling by registration of multiple range images, *Image and Vision Computing*, 10(3):145–155.

Derpanis, K.G., 2010. *Overview of the RANSAC Algorithm*, Technical report, Computer Science, York University, May 2010, URL: *http://www.cse.yorku.ca/~kosta/CompVis_Notes/ransac.pdf* (last date accessed: 02 September 2014).

Dold, C., and C. Brenner, 2006. Registration of terrestrial laser scanning data using planar patches and image data, *International Archives of Photogrammetry, Remote Sensing and Spatial Information Sciences*, 36(5):78–83.

Habib, A., K.I. Bang, A.P. Kersting, and J. Chow, 2010. Alternative Methodologies for LiDAR System Calibration, *Remote Sensing*, 2(3):874–907.

Habib, A., I. Detchev, and K. Bang, 2010. Comparative analysis of two approaches for multiple-surface registration of irregular point clouds, *International Archives of the Photogrammetry, Remote Sensing and Spatial Information Sciences(ISPRS)*, Commission I Mid-Term Symposium Proceedings, Calgary, Canada, 15-18 June, Vol., XXXVIII, Part1.

Habib, A., M. Ghanma, M. Michel, and R. Al-Ruzouq, 2005. Photogrammetric and lidar data registration using linear features, *Photogrammetric Engineering & Remote Sensing*, 71(6):699–707.

Habib, A.F., and R.I. Al-Ruzouq, 2004. Line-based modified iterated Hough transform for automatic registration of multi-source imagery, The Photogrammetric Record, 19(105):5–21.

Jaw, J., and T. Chuang, 2008. Feature-based registration of terrestrial LiDAR point clouds, *International Archives of the Photogrammetry, Remote Sensing and Spatial Information Sciences (ISPRS)*, Beijing, China, Vol. XXXVII. Part B3b, pp. 303–308.

Kang, Z., J. Li, L. Zhang, Q. Zhao, and S. Zlatanova, 2009. Automatic registration of terrestrial laser scanning point clouds using panoramic reflectance images, *Sensors*, 9(4):2621–2646.

Lari, Z., and A. Habib, 2013. A novel hybrid approach for the extraction of linear/cylindrical features from laser scanning data, *ISPRS Annals of Photogrammetry, Remote Sensing and Spatial Information Sciences, ISPRS Workshop Laser Scanning 2013*, 11-13 November, Antalya, Turkey, Vol.II-5/W2, pp. 151–156.

Lari, Z., A. Habib, and E. Kwak, 2011. An adaptive approach for segmentation of 3D laser point cloud, *International Archives of the Photogrammetry, Remote Sensing and Spatial Information Sciences (ISPRS)*, Calgary, AB, Canada, pp. 103–108.

Liang, Y.-B., Q.-M. Zhan, E.-Z. Che, M.-W. Chen, and D.-L. Zhang, 2014. Automatic registration of terrestrial laser scanning data using precisely located artificial planar targets, *Geoscience and Remote Sensing Letters (IEEE)*, 11(1):69–73.

Matabosch, C., J. Salvi, D. Fofi, and F. Meriaudeau, 2005. Range image registration for industrial inspection, *Proceedings of Machine Vision Applications in Industrial Inspection XIII*, San Jose, California, SPIE, 5679, pp. 216–227.

Rabbani, T., and F. van den Heuvel, 2005. Automatic point cloud registration using constrained search for corresponding objects, *Proceedings of 7th Conference on Optical 3-D Measurement Techniques*, 03-05 October, Vienna, Austria, pp. 177–186.

Renaudin, E., A. Habib, and A.P. Kersting, 2011. Featured-based registration of terrestrial laser scans with minimum overlap using photogrammetric data, *Electronics and Telecommunications Research Institute (ETRI) Journal*, 33(4):517–527.

Roberts, K.S., 1988. A new representation for a line, *Proceedings of Computer Vision and Pattern Recognition, Computer Society Conference*, pp. 635–640.

Theiler, P., and K. Schindler, 2012. Automatic registration of terrestrial laser scanner point clouds using natural planar surfaces, *ISPRS Annals of the Photogrammetry, Remote Sensing and Spatial Information Sciences*, XXII ISPRS Congress, 25 August-01 September 2012, Melbourne, Australia, Volume I-3, pp. 173–178.

Wen, C., L. Qin, Q. Zhu, C. Wang, and J. Li, 2014. Three-dimensional indoor mobile mapping with fusion of two-dimensional laser scanner and RGB-D camera data, *Geoscience and Remote Sensing Letters (IEEE)*, 11(4):843–847.

Wilkinson, B.E., A.H. Mohamed, B.A. Dewitt, and G.H. Seedahmed, 2010. A novel approach to terrestrial lidar georeferencing, Photogrammetric Engineering & Remote Sensing, 76(6):683–690.

Yao, J., M.R. Ruggeri, P. Taddei, and V. Sequeira, 2010. Automatic scan registration using 3D linear and planar features, *3D Research*, 1(3):1–18.

Zaharescu, A., E. Boyer, K. Varanasi, and R. Horaud, 2009. Surface feature detection and description with applications to mesh matching, *Proceedings of Computer Vision and Pattern Recognition, CVPR 2009 IEEE Conference*, Miami, Florida, 20-25 June, pp. 373–380.

Zhang, Z., 1994. Iterative point matching for registration of free-form curves and surfaces, *International Journal of Computer Vision*, 13(2):119–152.

(Received 14 March 2014; accepted 20 May 2014; final version 13 June 2014)